Distribution of Ni, Zn and Au in the interfacial intermetallic layer of micro-alloyed Sn-0.7Cu-0.05Ni /Cu BGA solder joints

G. Zeng[a], S. D. McDonald[a], D.K. Mu[b], Y. Terada[c] and K. Nogita[a]

[a]Nihon Superior Centre for the Manufacture of Electronic Materials(NS CMEM), School of Mechanical and Mining Engineering, The University of Queensland, St Lucia, QLD 4072, Australia;
[b]Nihon Superior Co. Ltd., Suita-City, Osaka 564-0063, Japan;
[c]The Japan Synchrotron Radiation Research Institute, Sayo-cho, Hyogo 679-5148, Japan

This study investigates the distribution of Ni, Zn and Au in the interfacial Cu_6Sn_5 layer and adjacent areas of micro-alloyed Sn-0.7Cu-0.05Ni/Cu BGA joints using synchrotron micro X-ray fluorescence analysis. Elemental distributions were characterized both before and after ageing for 500h at 150°C. The results show that Ni has a higher concentration on the side closest the Cu substrate before and after annealing. All three elements, Ni, Zn and Au are strongly concentrated within the interfacial Cu_6Sn_5 layer. The presence of Zn and Au within the Cu_6Sn_5 layer supports observations that these elements act in a similar way to Ni in the crystallographic stabilization of Cu_6Sn_5, which has been associated with increased reliability and integrity of BGA joints.

Keywords: Micro-XRF mapping, Intermetallics, Solders

Background and aim:

Ni is one of the most effective elements used as an additive in lead-free solder alloys and has been shown to significantly improve the properties of Sn-0.7 wt.%Cu solders [1-30]. Trace amount of Ni (0.05 wt.%) can significantly modify the eutectic structure and increase the fluidity during solidification [19]. Moreover, as discovered by Nogita et al., using synchrotron PXRD, transmission electron microscopy (TEM) and differential scanning calorimetry (DSC), the hexagonal structure of Cu_6Sn_5 in lead-free solder alloys and joints with trace Ni additions is very stable over a wide temperature range of -80 to 240°C[2, 4, 11, 13, 20, 21]. The polymorphic phase transformation of hexagonal to monoclinic in Cu_6Sn_5 is inhibited by doping with Ni. The improvement in properties may be related to Ni substituting Cu atoms in Cu_6Sn_5[11]. In summary, Ni is a very effective micro-alloying element and has a significant influence on the solidification behaviour of Sn-Cu alloys and also on the characteristics of intermetallics in solder joints. As electronic devices become more complicated and smaller, there has been a paradigm shift from 2-D to 3-D integrated circuit (3D ICs) architecture[31]. In these 3D ICs the size of the joint may decrease so much that the properties are dominated by the intermetallic that forms at the soldered interface, i.e. the parent solder material is almost entirely consumed in the soldering process. This necessitates a deeper understanding of the microstructural stability of interfacial IMC and the effect of minor elements on IMC formation and properties, even in well established alloys such as Sn-0.7Cu-0.05Ni. Micro-alloying is generally considered to be one of the most efficient ways to modify the microstructure and improve the performance of lead-free solders. Similar to the disproportionate effect that small quantities of Ni have on the properties of Sn-0.7Cu solders, Zn and Au are both found to be very promising candidate elements capable of improving the reliability of Sn-0.7Cu-0.05Ni solders[5, 7, 9, 15, 32-41]. In our recent study, the elements Zn and Au, which both exhibit marked solubility in Cu_6Sn_5, were shown to stabilise hexagonal Cu_6Sn_5 avoiding the polymorphic phase transformation that occurs in similar binary Sn-Cu alloys[15, 40]. Therefore, the stability of the interfacial intermetallic layer has been improved by avoiding this polymorphic phase transformation and the volume change induced by this transformation can be suppressed. However, there are still a lot of unresolved questions about the effects of Zn and Au on interfacial reactions between the solder and substrate, and specifically there is little information available in the literature detailing the distribution of Zn and Au within Cu_6Sn_5 directly after soldering and how this changes during subsequent annealing. This information is an essential aspect in understanding solder joint reliability, and will facilitate future solder alloy design.

Experimental:

Three compositions of solder alloys in the form of ball grid arrays (BGAs) were prepared, i.e.,

Sn-0.7Cu-0.05Ni, Sn-0.7Cu-0.07Au-0.06Ni, and Sn-0.7Cu-0.06Zn-0.05Ni (all in wt.%). The diameter of the BGA ball is around 500 μm. The test samples were reflowed on organic solderability preservative (OSP)-finished 30 μm thick Cu plating on FR-4 printed circuit boards (PCBs) by contact bonding. These samples experienced two reflows (a peak temperature of 250°C as specified in reflow temperature profile in Figure 1) and half of the samples were also subjected to annealing at 150°C for 500h after 2 reflows. After reflow and subsequent annealing, samples were embedded into resin and polished down to ~100 μm, along the cross-sectional direction to the solder interface, using conventional grinding and polishing techniques for sample preparation.

The μ-XRF experiment was been carried out at the undulator beamline BL37XU of the SPring-8 synchrotron. The undulator radiation X-rays are monochromatized with a Si 111 double-crystal monochromator. The rotated-inclined geometry is used to manage high heat-loads from the undulator radiation. The pin-post crystal is used as the first crystal and cooled by water directly, while the second crystal is cooled indirectly. The focusing optics is located at 57 m from the light source while the vertical source is determined by the electron beam in the undulator. The horizontal source size is defined by an XY slit placed at 34 m from the light source. The diffraction limited spot size determined by the numerical aperture is 0.19 mm (V)×0.15 mm (H) at 30 keV. The effective length of each mirror is about 90% of the full length, because the platinum coating shows relatively thin thickness at the either marginal area of the mirrors. In the focusing experiment, the illuminating beam size is determined by a 4-jaws slit in front of the mirror, and only the center area of the mirror (90 mm for each mirror) is illuminated. The micro-focusing optics were adopted in a scanning X-ray microprobe system. The sample consisting of a polished thin sections of solder joints is mounted on an XY stage, and a fluorescent X-ray take off angle of 10° is usually used for the XRF experiments. An energy dispersive Si (Li) solid state detector, was used to measure the fluorescence signal from the sample, and placed perpendicular to the incident beams to minimize the X-rays scattered from the sample. The measurements were conducted at the X-ray energy of 12 keV. The data was processed and analysed using Igor 6.32A software.

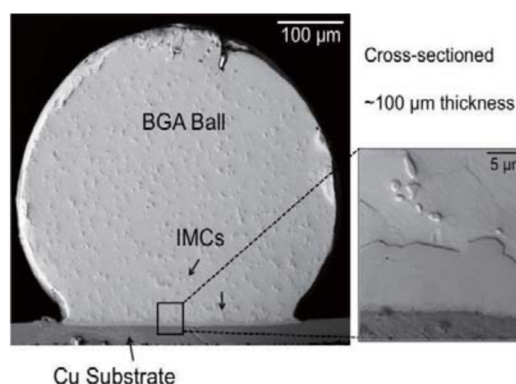

Figure 1. BGA solder joints.

Results and discussion:

Firstly in order to accurately measure the distribution of trace alloying elements, the energy dispersive spectrum (EDS) obtained from μ-XRF needs to be decomposed to eliminate the influence of strong peaks arising from the major/ultra-high concentration elements (i.e. CuKα and CuKβ) in the sample. For instance, as illustrated in point EDS analysis of Figure 2(b), the peaks of CuKα and CuKβ have a great influence on the ZnKα peaks. The correction procedure is as follows,

1. Determine the intensity of background of the EDS spectrum, assumed to be constant, proportional to the intensity of CuKα and also independent of channels/energy.
2. Use Gaussian functions to fit each peak of the EDS spectrum, and then refine the parameters of the Gaussian functions to minimise the differential between the modelling and measured spectrums.
3. Apply the parameters obtained in Step 2 to the dataset of μ-XRF mapping, to modify the intensity of each element/channel in mapping (to eliminate the interference contributed by strong peaks of other elements). In this way the corrected μ-XRF mapping can be obtained and plotted.
4. Verify the modified mapping results by obtaining other spectrums from different locations to make sure the corrected intensity of elements have realistic values.

After correction, distribution of trace alloying elements along the interface is displayed. The interface of the solder joint can be divided into three parts: the Cu substrate, interfacial layer and solder matrix. The thickness of the interfacial IMC layer increased from ~2 μm in reflowed condition to ~6-8 μm with 500h annealing. Generally speaking, Cu, Sn, Ni, Au and Zn elements were present in the interfacial layer. It is widely confirmed that the interfacial phase of the Sn/Cu couple is Cu_6Sn_5[42]. In this experiment, it can be clearly seen that elements of Ni, Au and Zn all have a strong concentration in the interfacial Cu_6Sn_5

intermatallics (IMC) layer with/without annealing.

Au was also found to accumulate within interfacial Cu_6Sn_5, as shown in Figure 2. In reflowed Sn-0.7Cu-0.07Au-0.06Ni BGA joints, the concentration of Ni is much higher than Au within interfacial Cu_6Sn_5. Different from the above mentioned two samples Sn-0.7Cu-0.05Ni and Sn-0.7Cu-0.06Zn-0.05Ni, Ni is found more homogeneously distributed in interfacial Cu_6Sn_5 in the as-reflowed state. After 500h of annealing, Ni became more inhomogeneous in Cu_6Sn_5 but there were more Ni-rich zones appearing near the side adjacent the solder matrix. Au concentration remained stable after annealing and was still relatively homogeneous in the interfacial Cu_6Sn_5.

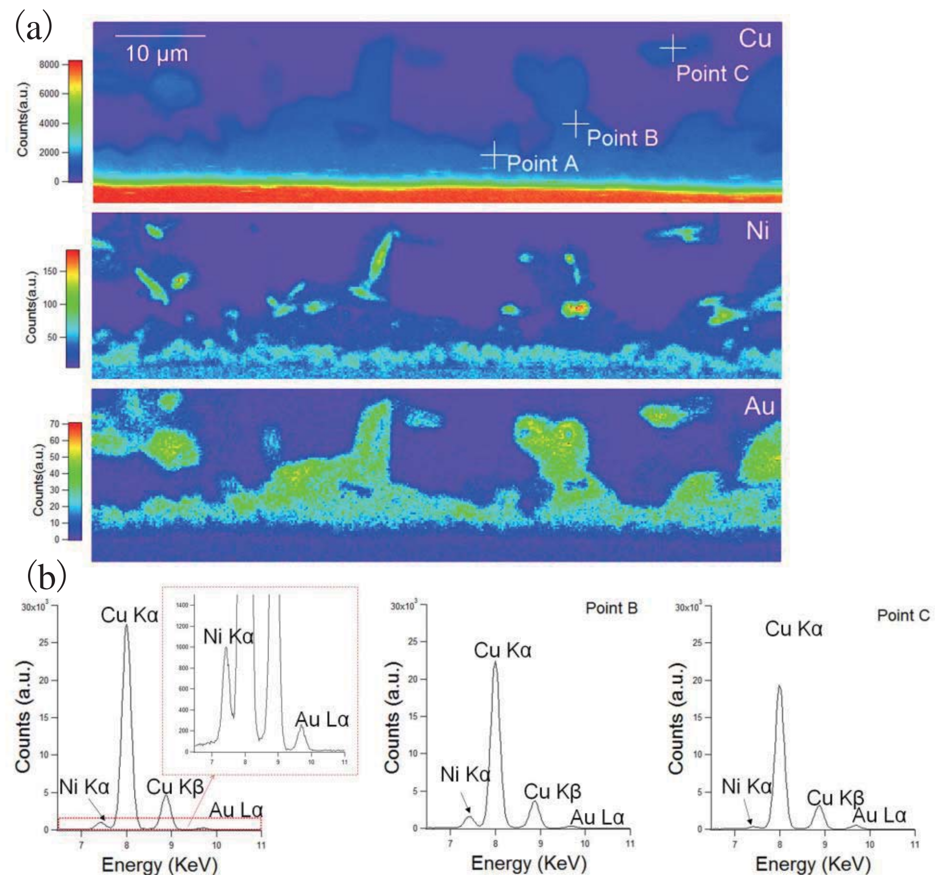

Figure 2. μ-XRF measurement of interfacial region in Sn-0.7Cu-0.07Au-0.06Ni/Cu solder joint; (a) mapping of Cu, Ni, Au (scan pitch: 200 nm, exposure time: 0.3 s); (b) XRF spectrums from Position A, B, and C in (a) of 500h annealed Sn-0.7Cu-0.06Au-0.05Ni/Cu (exposure time: 60 s).

Conclusions and future works:

The results of this experiment, revealed the distribution of trace alloying elements Ni, Zn and Au in interfacial Cu_6Sn_5 layers of micro-alloyed Sn-0.7Cu-0.05Ni BGA joints for the first time. Based on our previously finding and the present results, it is believed that Zn and Au extend the ability of Ni to stabilise the interfacial Cu_6Sn_5, further enhancing the reliability and integrity of BGA solder joints. Currently, studies about influences of Zn, Au and Ni on the phase stability of interfacial Cu_6Sn_5 and the thermal expansion misfit between Cu_6Sn_5 and Cu substrates, for industrially relevant solder joints, are being conducted using synchrotron XRD and Transmission Electron Microscopy (TEM).

Acknowledgments:

We gratefully acknowledge financial support from the University of Queensland-Nihon Superior collaborative research program. Synchrotron micro XRF mapping were performed at the Japan Synchrotron Radiation Research Institute (JASRI) on BL37XU of the SPring-8 synchrotron, under Proposal No.2013B1524. The authors thank Mr. J. Read of The University of Queensland for valuable discussions, and Prof. Hideyuki Yasuda from Kyoto University for valuable discussions and experimental assistance. G. Zeng is financially supported by a University of Queensland International (UQI) Scholarship and a China Scholarship Council (CSC) Scholarship.

References:

[1] K. Nogita, C. Gourlay, T. Nishimura, *JOM* 61 (2009) 45-51.
[2] Y.Q. Wu, S.D. McDonald, J. Read, H. Huang, K. Nogita, *Scripta Materialia*, 68 (2013) 595-598.
[3] S.H. Huh, K.S. Kim, K. Suganuma, *Materials Transactions, JIM*, 43 (2002) 239-245.
[4] K. Nogita, D. Mu, S.D. McDonald, J. Read, Y.Q. Wu, *Intermetallics*, 26 (2012) 78-85.
[5] M.G. Cho, S.K. Kang, D.Y. Shih, H.M. Lee, *Journal of Electronic Materials*, 36 (2007) 1501-1509.
[6] A.A. El-Daly, A.M. El-Taher, T.R. Dalloul, *Materials & Design*, 55 (2014) 309-318.
[7] A.A. El-Daly, A.M. El-Taher, *Materials & Design*, 51 (2013) 789-796.
[8] C. Yang, F. Song, S.W. Ricky Lee, *Microelectronics Reliability*, 54 (2014) 435-446.
[9] T. Laurila, V. Vuorinen, M. Paulasto-Kröckel, *Materials Science and Engineering Reports*, 68 (2010) 1-38.
[10] C.M. Gourlay, K. Nogita, A.K. Dahle, Y. Yamamoto, K. Uesugi, T. Nagira, M. Yoshiya, H. Yasuda, *Acta Materialia*, 59 (2011) 4043-4054.
[11] U. Schwingenschlogl, C. Di Paola, K. Nogita, C. Gourlay, *Applied Physics Letters*, 96 (2010) 061908.
[12] K.-C. Huang, F.-S. Shieu, Y.H. Hsiao, C.Y. Liu, *Journal of Electronic Materials*, 41 (2012) 172-175.
[13] K. Nogita, T. Nishimura, *Scripta Materialia*, 59 (2008) 191-194.
[14] R. Gagliano, G. Ghosh, M. Fine, *Journal of Electronic Materials*, 31 (2002) 1195-1202.
[15] G. Zeng, S.D. McDonald, Q. Gu, S. Suenaga, Y. Zhang, J. Chen, K. Nogita, *Intermetallics*, 43 (2013) 85-98.
[16] G. Ghosh, M. Asta, *Journal of Materials Research*, 20 (2005) 3102-3117.
[17] M. Li, Z. Zhang, J. Kim, *Applied Physics Letters*, 98 (2011) 201901-201901-201903.
[18] Y.-H. Wu, C.-Y. Yu, C.-Y. Ho, J.-G. Duh, *Materials Letters*, 105 (2013) 40-42.
[19] C.M. Gourlay, K. Nogita, S.D. McDonald, T. Nishimura, K. Sweatman, A.K. Dahle, *Scripta Materialia*, 54 (2006) 1557-1562.
[20] K. Nogita, *Intermetallics*, 18 (2010) 145-149.
[21] D. Mu, J. Read, Y. Yang, K. Nogita, *J Mater Res* 26 (2011) 2660-2664.
[22] S.W. Chen, S.H. Wu, S.W. Lee, *J Electron Mater* 32 (2003) 1188-1194.
[23] M. Felberbaum, T. Ventura, M. Rappaz, A. Dahle, *JOM* 63 (2011) 52-55.
[24] C.M. Gourlay, K. Nogita, J. Read, A.K. Dahle*, J Electron Mater* 39 (2010) 56-69.
[25] C.M. Gourlay, J. Read, K. Nogita, A.K. Dahle, *J Electron Mater* 37 (2008) 51-60.
[26] M.J. Rizvi, C. Bailey, Y.C. Chan, M.N. Islam, H. Lu, *Journal of Alloys and Compounds*, 438 (2007) 122-128.
[27] M.J. Rizvi, C. Bailey, Y.C. Chan, H. Lu, *Proc. 1st Electronics Systemintegration Technology Conference*, (2006) 145-251.
[28] M.J. Rizvi, C. Bailey, Y.C. Chan, H. Lu, *Journal of Alloys and Compounds*, 438 (2007) 116-121.
[29] T. Ventura, Y.-H. Cho, C. Kong, A.K. Dahle, *J Electron Mater* 40 (2011) 1403-1408.
[30] G. Zeng, S. Xue, L. Zhang, L. Gao, J Mater Sci: *Mater Electron*, 22 (2011) 565-578.
[31] H. Lin, C. Lu, C. Liu, C. Chen, D. Chen, J. Kuo, K.N. Tu, *Acta Materialia*, 61 (2013) 4910-4919.
[32] C.Y. Chou, S.W. Chen, *Acta Materialia*, 54 (2006) 2393-2400.
[33] T. El-Ashram, R. Shalaby, *J Electron Mater* 34 (2005) 212-215.
[34] S. Kang, D.-Y. Shih, D. Leonard, D. Henderson, T. Gosselin, S.-i. Cho, J. Yu, W. Choi, *JOM*, 56 (2004) 34-38.
[35] W.Q. Shao, C.Y. Yu, W.C. Lu, J.G. Duh, S.O. Chen, *Materials Letters*, 93 (2013) 300-303.
[36] F. Wang, X. Ma, Y. Qian, *Scripta Materialia*, 53 (2005) 699-702.
[37] S.C. Yang, C.E. Ho, C.W. Chang, C.R. Kao, *Journal of Materials Research*, 21 (2011) 2436-2439.
[38] C.Y. Yu, J.G. Duh, *Scripta Materialia*, 65 (2011) 783-786.
[39] G. Zeng, S.D. McDonald, C.M. Gourlay, K. Uesugi, Y. Terada, H. Yasuda, K. Nogita, *Metall Mater Trans A* (2013) 1-9.
[40] G. Zeng, S.D. McDonald, Q. Gu, K. Nogita, *J Mater Res* 27 (2012) 2609-2614.
[41] S.H. Huh, K.S. Kim, K. Suganuma, *Mater Trans*, 43 (2002) 239-245.
[42] T. Laurila, V. Vuorinen, M. Paulasto-Kröckel, *Materials Science and Engineering: R*: Reports, 68 (2010) 1-38.